# What Every Radiologist Should Know about Idiopathic Interstitial Pneumonias[1]

**RadioGraphics**

**LEARNING OBJECTIVES FOR TEST 1**

*After reading this article and taking the test, the reader will be able to:*

- List the seven entities included in the ATS-ERS classification of IIPs.

- Describe the morphologic patterns associated with the IIPs.

- Identify these patterns at high-resolution CT and interpret them in the appropriate clinicopathologic context.

**TEACHING POINTS**

*See last page*

*Christina Mueller-Mang, MD • Claudia Grosse, MD • Katharina Schmid, MD • Leopold Stiebellehner, MD • Alexander A. Bankier, MD*

The American Thoracic Society–European Respiratory Society classification of idiopathic interstitial pneumonias (IIPs), published in 2002, defines the morphologic patterns on which clinical-radiologic-pathologic diagnosis of IIPs is based. IIPs include seven entities: idiopathic pulmonary fibrosis, which is characterized by the morphologic pattern of usual interstitial pneumonia (UIP); nonspecific interstitial pneumonia (NSIP); cryptogenic organizing pneumonia (COP); respiratory bronchiolitis–associated interstitial lung disease (RB-ILD); desquamative interstitial pneumonia (DIP); lymphoid interstitial pneumonia (LIP); and acute interstitial pneumonia (AIP). The characteristic computed tomographic findings in UIP are predominantly basal and peripheral reticular opacities with honeycombing and traction bronchiectasis. In NSIP, basal ground-glass opacities tend to predominate over reticular opacities, with traction bronchiectasis only in advanced disease. COP is characterized by patchy peripheral or peribronchovascular consolidation. RB-ILD and DIP are smoking-related diseases characterized by centrilobular nodules and ground-glass opacities. LIP is characterized by ground-glass opacities, often in combination with cystic lesions. AIP manifests as diffuse lung consolidation with ground-glass opacities, which usually progress to fibrosis in patients who survive the acute phase of the disease. Correct diagnosis of IIPs can be achieved only by means of interdisciplinary consensus and stringent correlation of clinical, imaging, and pathologic findings.
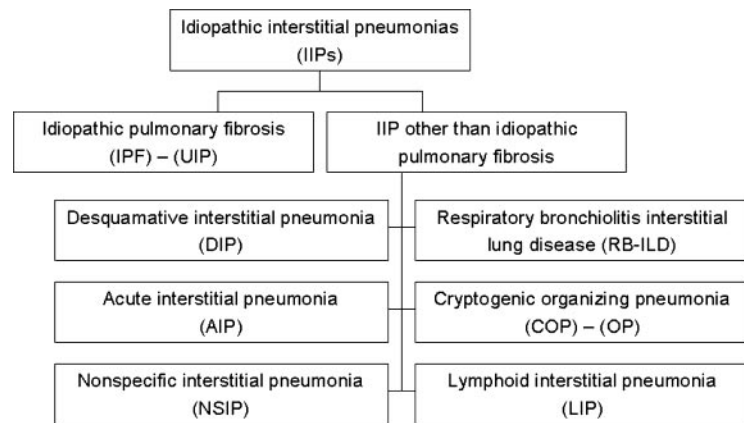
©RSNA, 2007

©RSNA, 2007

**Figure 1.**   Terminology for the IIPs with the various subentities according to the ATS-ERS classification. *UIP* = usual interstitial pneumonia.

**Table 1**
**Clinical Features of Patients with IIPs according to the ATS-ERS Consensus Statement**

| Type of IIP | Mean Age at Onset (y) | Gender Distribution | Most Prominent Symptoms | Type of Onset | Association with Smoking | Prognosis | Response to Corticosteroids |
|---|---|---|---|---|---|---|---|
| IPF | >50 | More common in men | Dyspnea, cough | Gradual | Currently under discussion | Poor (median survival, 2.5–3.5 y) | Poor, if any |
| NSIP | 40–50 | Equal | Dyspnea, cough, fatigue | Gradual or subacute | None | Variable, better than in UIP | Good |
| COP | 55 | Equal | Cough, mild dyspnea, fever | Subacute | More common in nonsmokers | Complete recovery in most patients | Excellent |
| RB-ILD | 30–40 | More common in men | Mild dyspnea, cough | Gradual | Required for diagnosis | Good after smoking cessation | Good |
| DIP | 30–40 | More common in men | Dyspnea, cough | Insidious | In most cases | Generally good after smoking cessation | Good |
| LIP | 40–50 | More common in women | Cough, dyspnea | Slow | None | Variable | Variable |
| AIP | 50 | Equal | Dyspnea | Acute | None | High mortality rate (≥50%) | Not proved |

Source.—Reference 3.

## Introduction

The diagnostic approach to idiopathic interstitial pneumonias (IIPs) has long been confusing because these disorders were categorized according to different clinical, radiologic, and histologic classifications (1,2).

In 2001, the American Thoracic Society (ATS) and European Respiratory Society (ERS) standardized the terminology for IIPs (Fig 1) (3). This new ATS-ERS classification is the result of a multidisciplinary consensus and includes seven disease entities: idiopathic pulmonary fibrosis (IPF), nonspecific interstitial pneumonia (NSIP), cryptogenic organizing pneumonia (COP), respiratory bronchiolitis–associated interstitial lung

**Table 2**
**Histopathologic and CT Features of IIPs**

| Morphologic Pattern | Histopathologic Features | Distribution at CT | High-Resolution CT Features |
|---|---|---|---|
| UIP | Spatial and temporal heterogeneity, architectural distortion, fibroblastic foci | Apicobasal gradient, subpleural | Macrocystic honeycombing, reticular opacities, traction bronchiectasis, architectural distortion, focal ground-glass opacity |
| NSIP | Spatial and temporal homogeneity; cellular pattern shows mild to moderate interstitial chronic inflammation; fibrosing pattern shows dense or loose interstitial fibrosis | No obvious gradient, subpleural, symmetric | Ground-glass opacities, irregular linear or reticular opacities, micronodules, consolidation, microcystic honeycombing |
| COP | Patchy distribution of intraluminal organizing fibrosis in distal airspaces, preservation of lung architecture, uniform temporal appearance | Patchy, peripheral or peribronchial, basal predominance, sometimes sparing of subpleural space, migration tendency | Airspace consolidation, mild bronchial dilatation, ground-glass opacities, large nodules (rare) |
| RB-ILD | Bronchiolocentric accumulation of alveolar macrophages containing brown particles, mild bronchiolar fibrosis | Diffuse or upper lung predominance | Centrilobular nodules, patchy ground-glass opacities, bronchial wall thickening |
| DIP | Diffuse accumulation of macrophages in distal airspaces, mild interstitial fibrosis, mild chronic inflammation | Apicobasal gradient, peripheral predominance | Ground-glass opacities, irregular linear or reticular opacities, sometimes cysts |
| LIP | Diffuse infiltration of alveolar septa by lymphoid cells, lymphoid hyperplasia frequent | Basilar predominance or diffuse | Ground-glass opacities, perivascular cysts, septal thickening, centrilobular nodules |
| AIP | Diffuse alveolar damage; exudative phase shows hyaline membranes, diffuse alveolar infiltration by lymphocytes; organizing phase shows alveolar wall thickening due to fibrosis, pneumocyte hyperplasia | Lower lung predominance, symmetric, bilateral | Exudative phase shows ground-glass opacities, airspace consolidation; organizing phase shows bronchial dilatation, architectural distortion |

disease (RB-ILD), desquamative interstitial pneumonia (DIP), lymphoid interstitial pneumonia (LIP), and acute interstitial pneumonia (AIP).

In their idiopathic form, IIPs are rare diseases. However, more frequent disorders such as sarcoidosis, vasculitis, and connective tissue diseases can display identical morphologic patterns, and the IIPs are considered "prototypes" for these morphologic alterations (3). Because imaging plays a crucial role in identifying both the idiopathic and the secondary interstitial pneumonias, radiologists need to be familiar with the morphologic and clinical manifestations and the diagnostic approach to these conditions.

The main clinical symptoms of IIPs are nonspecific and consist of cough and dyspnea; however, other factors such as age, gender, risk factors, and course of disease can be helpful in distinguishing between the various entities (Table 1).

The classification of IIPs is based on histologic criteria, but each histologic pattern is associated with a characteristic computed tomography (CT) pattern that, provided an adequate CT technique is used, correlates well with histologic findings (Table 2) (3).
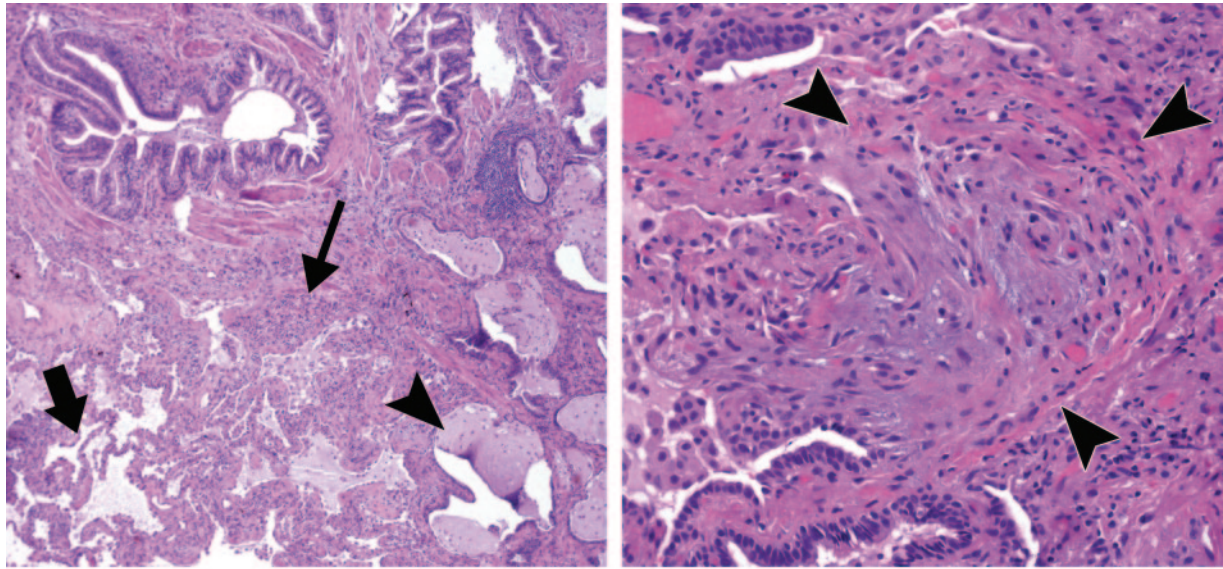
**Teaching Point**

**Figure 2.** Histologic features of UIP. **(a)** Photomicrograph (original magnification, ×40; hematoxylin-eosin stain) shows patchy fibrosis with remodeling of the lung architecture. Interstitial chronic inflammation is mild, with only a few lymphoid aggregates (thin arrow). Cystically dilated airspaces that produce a honeycomb pattern (arrowhead) and areas of relatively unaffected lung (thick arrow) are present. **(b)** Photomicrograph (original magnification, ×200; hematoxylin-eosin stain) shows a fibroblastic focus of loose organizing connective tissue (arrowheads), which is the hallmark of UIP.

The key role that radiologists play in the work-up of IIPs necessitates a thorough knowledge of the patterns as described in the international classification and an increased awareness of the multidisciplinary challenges involved in their interpretation.

In this article, we illustrate the morphologic characteristics of the patterns included in the ATS-ERS classification of IIPs and present an encyclopedic review of the clinical and radiologic hallmarks associated with these patterns.

## Idiopathic Pulmonary Fibrosis

IPF is the most common entity of the IIPs. By definition, IPF is the term for the clinical syndrome associated with the morphologic pattern of UIP (3). With a median survival time ranging from 2 to 4 years, IPF has a substantially poorer prognosis than NSIP, COP, RB-ILD, DIP, and LIP (3,4).

### Clinical Features

The typical patient with IPF is 50 years old or older. Patients present with progressively worsening dyspnea and nonproductive cough (3). Many patients also report that the subtle onset of their symptoms months or even years earlier was mistaken for a less serious respiratory disease, which delayed referral to a specialized center (5). Although there are slightly more cases in men than in women, there is no obvious gender predilection (3). A history of cigarette smoking seems to be a risk factor for the development of IPF; however, it does not appear to affect the course of the disease (4,6,7). Usually, patients do not respond to high-dose corticosteroid therapy; data suggest that, due to the considerable side effects of corticosteroids, this therapy might even be contraindicated (8). However, a combination therapy of cyclosporin A and corticosteroids seems to be efficacious for acute exacerbations of IPF (9). In addition, patients should be considered candidates for lung transplantation early after diagnosis (10).
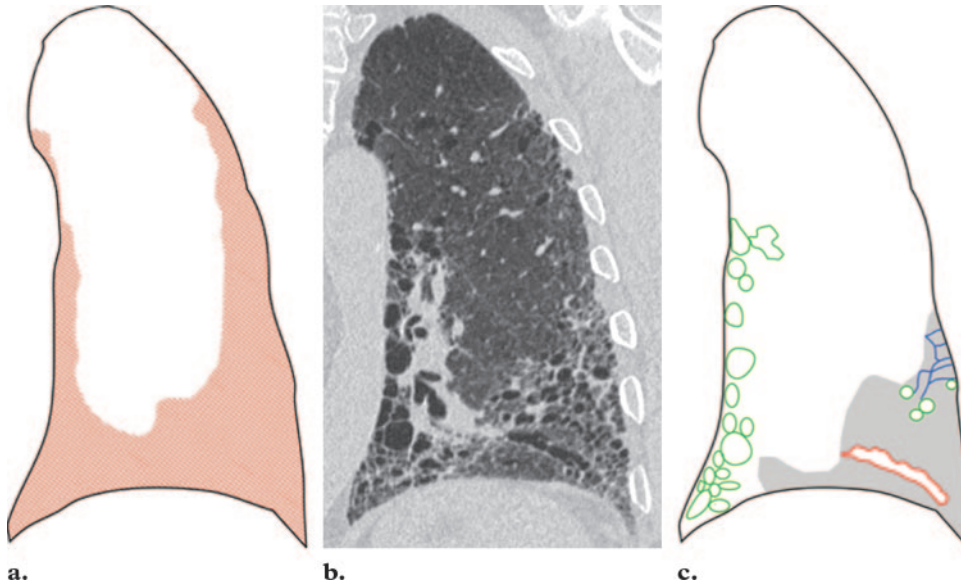
**Figure 3.**    Distribution **(a)**, CT image **(b)**, and CT pattern **(c)** of UIP. The distribution is subpleural with an apicobasal gradient (red area in **a**). CT shows honeycombing (green areas in **c**), reticular opacities (blue areas in **c**), traction bronchiectasis (red area in **c**), and focal ground-glass opacity (gray area in **c**).

## Histologic Features

The histologic hallmark of UIP is the presence of scattered fibroblastic foci (Fig 2). Typically, the lung involvement is heterogeneous and areas of normal lung alternate with interstitial inflammation and honeycombing (1). Owing to the patchy lung involvement, histologic evaluation of multiple biopsy specimens from one patient may reveal discordant histologic patterns. Evidence of the UIP pattern in one biopsy specimen is associated with a worse prognosis, independently of other coexisting patterns (11,12). Therefore, biopsy samples from more than one lobe should be obtained in any patient with suspected IIP, and high-resolution CT should serve as a guiding tool for determining the appropriate anatomic location of the biopsy site (12,13).

## Imaging Features

The chest radiograph is normal in most patients with early disease. In advanced disease, the chest radiograph shows decreased lung volumes and subpleural reticular opacities that increase from the apex to the bases of the lungs (14).

This apicobasal gradient is even better seen on high-resolution CT images. Together with subpleural reticular opacities and macrocystic honeycombing combined with traction bronchiectasis, the apicobasal gradient represents a trio of signs that is highly suggestive of UIP (Fig 3) (15,16). Therefore, UIP should be considered in patients who present with low lung volumes, subpleural reticular opacities, macrocystic honeycombing, and traction bronchiectasis, the extent of which increases from the apex to the bases of the lungs (Fig 4). In the typical patient with UIP, the disease is most extensive on the most basal section of the high-resolution CT examination. Ground-glass opacities are present in the majority of patients with UIP but are usually limited in extent (17). Typically, imaging findings are heterogeneous, with areas of fibrosis alternating with areas of normal lung (Fig 5).

**Teaching Point**

4a.

5a.



4b.

5b.
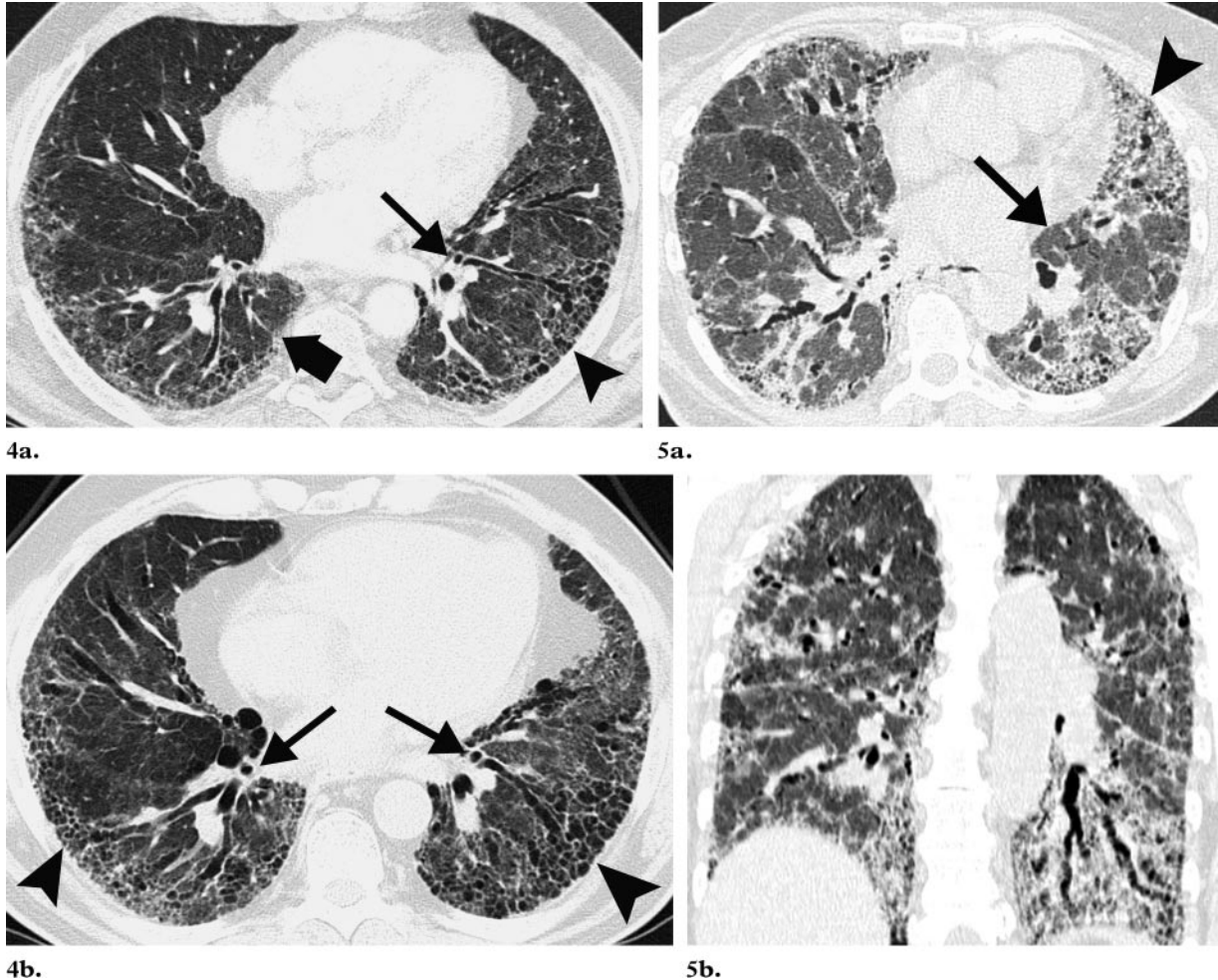
**Figures 4, 5.** **(4)** IPF in a 64-year-old man. **(a)** High-resolution CT image obtained at presentation shows reticular opacities, honeycombing (arrowhead), and focal ground-glass opacity (thick arrow). Moderate traction bronchiectasis is present (thin arrow). These findings are consistent with the UIP pattern. **(b)** Follow-up CT image obtained 12 months later shows marked progression of the honeycombing (arrowheads) and traction bronchiectasis (arrows). **(5)** IPF in a 67-year-old man. **(a)** High-resolution CT image shows areas of relatively unaffected lung parenchyma with only ground-glass opacity (arrow) next to fibrotic areas with honeycombing and traction bronchiectasis (arrowhead), an appearance typical of UIP. **(b)** Coronal CT image shows an obvious apicobasal gradient of the lung alterations.

In patients who show the characteristic distribution and high-resolution CT pattern of UIP and the appropriate clinical features, the diagnosis can be reliably made without biopsy (18,19). The ATS-ERS has defined eight major and minor criteria for the diagnosis of IPF in the absence of a surgical lung biopsy, which are summarized in Table 3. However, histologic confirmation should be obtained in all patients with atypical imaging findings, such as extensive ground-glass opacities, nodules, consolidation, or a predominantly peribronchovascular distribution (3,20).

### Nonspecific Interstitial Pneumonia

NSIP is less common than UIP but is still one of the most common histologic findings in patients with IIPs (21). NSIP is associated with a variety of imaging and histologic findings, and the diagnostic approach is highly challenging. However, the distinction of NSIP from UIP is more than academic, given the better response to corticosteroids seen in a subgroup of patients with NSIP (22,23).

Owing to the clinical, radiologic, and pathologic variability of NSIP, the term should be considered a provisional diagnosis until further characterization of this entity has been established (3).

### Clinical Features

The typical patient with NSIP is between 40 and 50 years old and is usually about a decade younger than the patient with IPF. Symptoms of NSIP are similar to those of IPF but usually milder (24). Patients present with gradually worsening dyspnea over several months, and they often experience fatigue and weight loss. There is no gender predilection, and cigarette smoking is not an obvious risk factor in the development of NSIP. Treatment of patients with NSIP is based
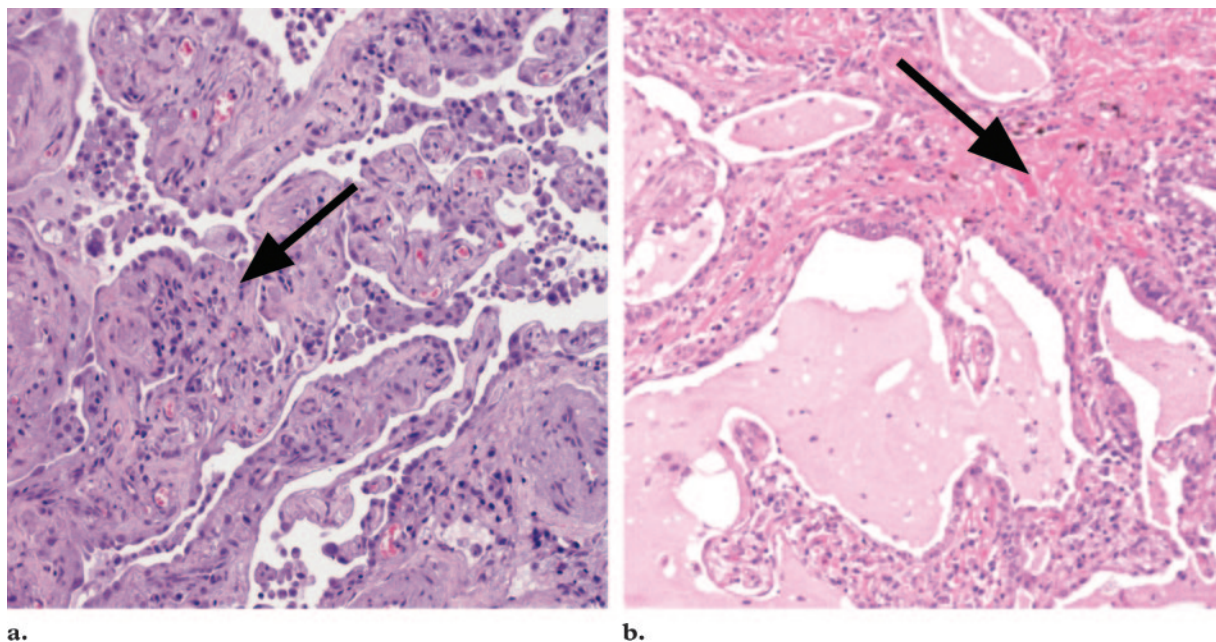
**Figure 6.** Histologic features of NSIP. **(a)** Photomicrograph (original magnification, ×100; hematoxylin-eosin stain) of cellular NSIP shows a uniform appearance of interstitial inflammation (arrow), which consists of lympho-cytes and plasma cells. **(b)** Photomicrograph (original magnification, ×100; hematoxylin-eosin stain) of fibrosing NSIP shows areas of fibrosis (arrow) in addition to uniform inflammation.

**Table 3**
**ATS-ERS Criteria for Diagnosis of IPF in the Absence of Surgical Lung Biopsy**

Major criteria
    Exclusion of other known causes of interstitial lung disease (eg, toxic effects of certain drugs, environmental ex-
        posures, and connective tissue diseases)
    Abnormal results of pulmonary function studies, including evidence of restriction (reduced vital capacity, often
        with an increased $FEV_1/FVC$ ratio) and impaired gas exchange (increased $P_{AO_2} - P_{aO_2}$, decreased $P_{aO_2}$ with
        rest or exercise, or decreased $D_{LCO}$)
    Bibasilar reticular abnormalities with minimal ground-glass opacities at high-resolution CT
    Transbronchial lung biopsy or bronchoalveolar lavage shows no features to support an alternative diagnosis
Minor criteria
    Age > 50 y
    Insidious onset of otherwise unexplained dyspnea on exertion
    Duration of illness > 3 mo
    Bibasilar inspiratory crackles (dry or "Velcro" type)

Source.—Reference 3.
Note.—$D_{LCO}$ = diffusing capacity of lung for carbon monoxide; $FEV_1$ = forced expiratory volume in 1 second; FVC = forced vital capacity; $P_{AO_2}$ = partial pressure of oxygen, alveolar; $P_{aO_2}$ = partial pressure of oxygen, arte-rial.

on the use of systemic corticosteroids in combina-tion with cytotoxic drugs, such as cyclophospha-mide and cyclosporin, and the majority of pa-tients stabilize or improve with this therapy (25).

Although it is primarily defined as an idio-pathic disease, the morphologic pattern of NSIP is encountered in association with frequent disor-ders, such as connective tissue diseases, hypersen-sitivity pneumonitis, or drug exposure (26,27). Once the morphologic pattern of NSIP has been determined in a patient, these secondary forms of NSIP must be ruled out by the clinician.

**Histologic Features**
The histologic pattern of NSIP is characterized by temporally and spatially homogeneous lung in-volvement (28). This homogeneity is a key feature in differentiating the NSIP pattern from the UIP pattern. On the basis of the varying proportions of inflammation and fibrosis, NSIP is divided into cellular and fibrosing subtypes (Fig 6) (1). In cel-lular NSIP, the thickening of alveolar septa is pri-marily caused by inflammatory cells; in fibrosing
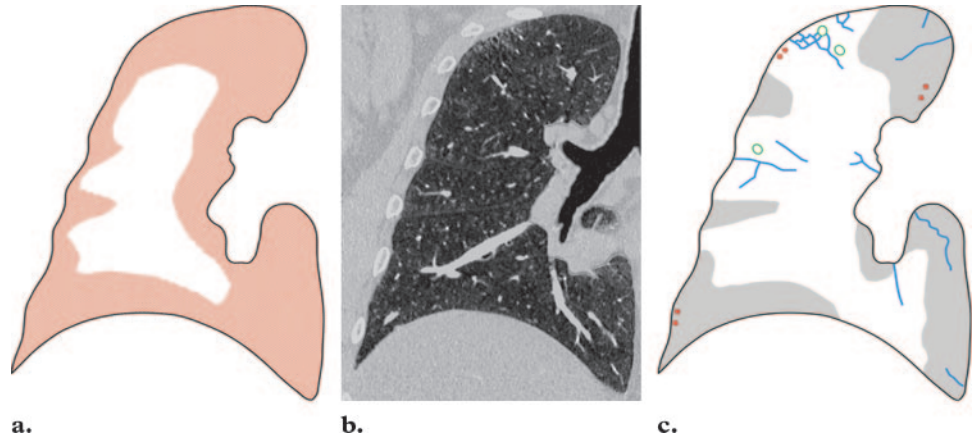
**Figure 7.**   Distribution **(a)**, CT image **(b)**, and CT pattern **(c)** of NSIP. The distribution is subpleural with no obvious gradient (red area in **a**). CT shows ground-glass opacity (gray areas in **c**), irregular linear and reticular opacities (blue areas in **c**), micronodules (red areas in **c**), and microcystic honeycombing (green areas in **c**).
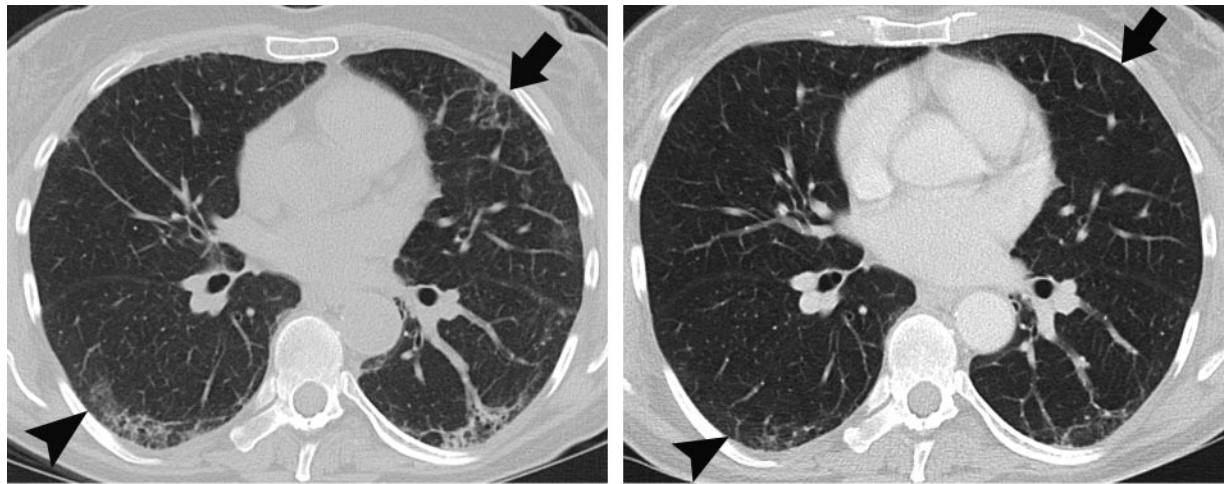


**Figure 8.**   NSIP in a 60-year-old woman with mild dyspnea and fatigue. **(a)** High-resolution CT image of the lower lungs shows bilateral subpleural ground-glass opacities (arrowhead) and irregular linear opacities (arrow). The patient received corticosteroid treatment. **(b)** Follow-up CT image obtained 6 months later shows improvement, with partial resolution of the ground-glass opacities (arrowhead) and linear opacities (arrow).
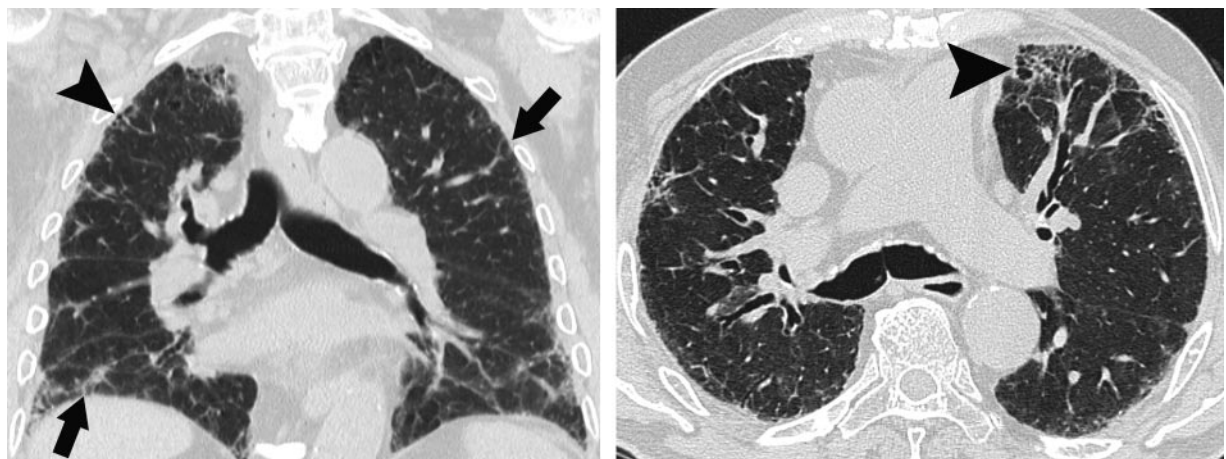


**Figure 9.**   NSIP in a 53-year-old man with mild dyspnea. **(a)** Coronal CT image shows diffuse lung involvement consisting of peripherally located irregular linear opacities with ground-glass opacities (arrows). Small cystic lesions are seen (arrowhead). **(b)** Axial high-resolution CT image shows the small cystic lesions more clearly (arrowhead).
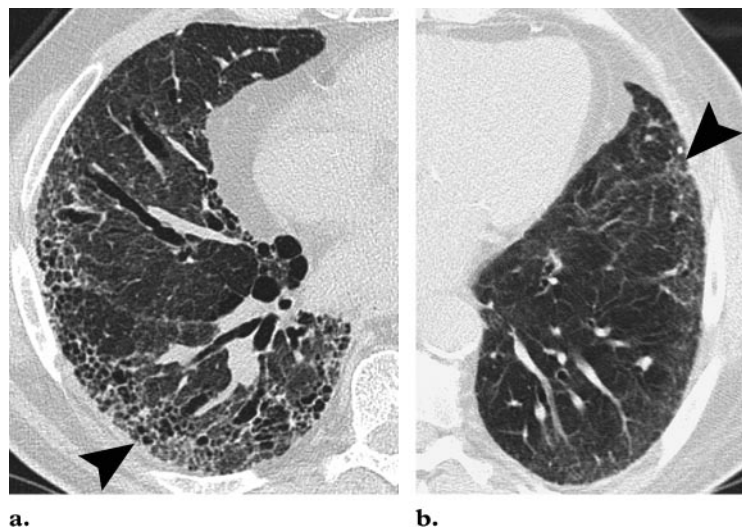
**Figure 11.** Comparison of high-resolution CT features between UIP and NSIP. **(a)** UIP is characterized by heterogeneous lung abnormalities consisting of subpleural honeycombing (arrowhead), reticular opacities, and traction bronchiectasis. **(b)** NSIP demonstrates homogeneous lung involvement with predominance of ground-glass opacity combined with subpleural linear opacities and micronodules. The microcysts in NSIP (arrowhead) are much smaller than the honeycombing in UIP.
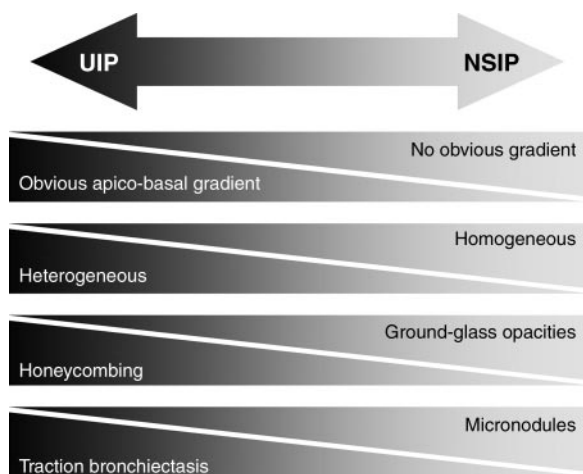


**Figure 10.** Key imaging features for differentiation between UIP and NSIP.

NSIP, interstitial fibrosis is seen in addition to mild inflammation. Cellular NSIP is less common than fibrosing NSIP but shows a better response to corticosteroids and carries a substantially better prognosis (21). Histologic distinction between fibrotic NSIP and UIP is difficult and is subject to substantial interobserver variation (20). In borderline cases, CT correlation may help by showing features more typical of either UIP or NSIP.

**Imaging Features**

In patients with early NSIP, the chest radiograph is normal. In advanced disease, bilateral pulmonary infiltrates are the most salient abnormality. The lower lung lobes are more frequently involved, but an obvious apicobasal gradient, as seen in UIP, is usually missing (3).

High-resolution CT typically reveals a subpleural and rather symmetric distribution of lung abnormalities (Fig 7). The most common manifestation consists of patchy ground-glass opacities combined with irregular linear or reticular opacities and scattered micronodules (Fig 8) (29–31). In advanced disease, traction bronchiectasis and consolidation can be seen; however, ground-glass opacities remain the most obvious high-resolution CT feature in the typical patient with NSIP and are related to the histologic finding of homogeneous interstitial inflammation (29,30).

Other findings in advanced NSIP include subpleural cysts, but compared to those of UIP, these cysts are smaller and limited in extent (Fig 9) (29). The term "microcystic honeycombing" is used for these cystic changes in NSIP, as opposed to the macrocystic honeycombing seen in UIP (32,33). Although the CT features of cellular and fibrotic NSIP overlap considerably, it has been shown that honeycombing is seen almost exclusively in patients with fibrotic NSIP (17,29). Other CT findings that have been correlated with increased likelihood of fibrosis in NSIP are the extent of traction bronchiectasis and intralobular reticular opacities (29).

Owing to the substantial overlap of high-resolution CT patterns, the major CT differential diagnosis for NSIP is UIP. The key CT features that favor the diagnosis of NSIP over UIP are homogeneous lung involvement without an obvious apicobasal gradient, extensive ground-glass abnormalities, a finer reticular pattern, and micronodules (Figs 10, 11) (17,20,34). Follow-up

**Figure 12.** Histologic features of COP. Photomicrograph (original magnification, ×100; hematoxylin-eosin stain) shows polypoid fibroblastic foci in the alveolar ducts and alveoli (arrows). The organizing connective tissue is all the same age and shows moderate cellular proliferation.
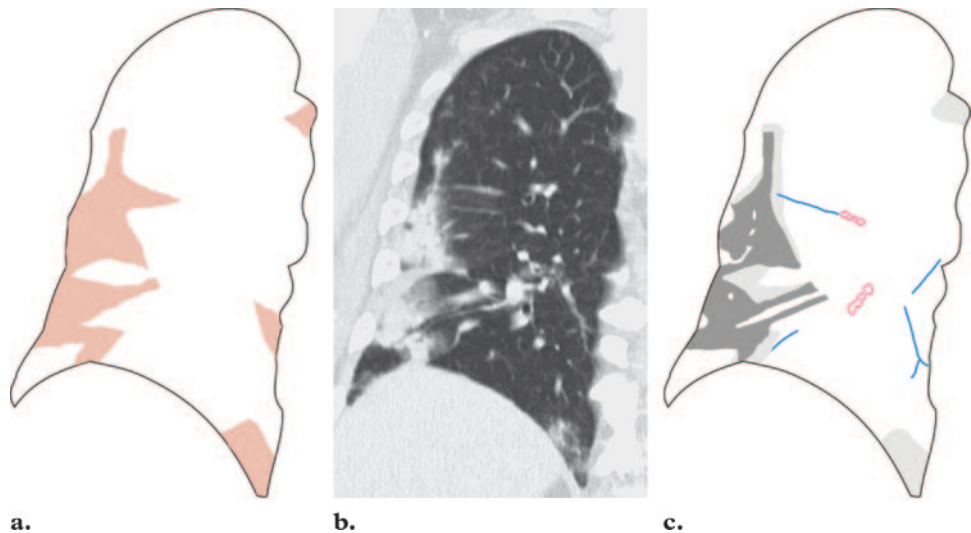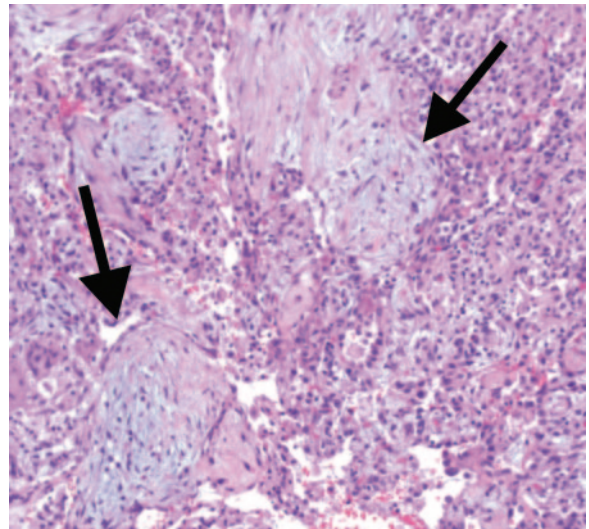


a.                              b.                              c.

**Figure 13.** Distribution **(a)**, CT image **(b)**, and CT pattern **(c)** of COP. The distribution is peripheral or peribronchial with a basal predominance (red areas in **a**). CT shows consolidation with air bronchograms (dark gray areas in **c**), ground-glass opacities (light gray areas in **c**), linear opacities (blue areas in **c**), and mild bronchial dilatation (red areas in **c**).

CT also demonstrates differences between patients with NSIP and those with UIP. In patients with NSIP, ground-glass opacities usually do not progress to areas of honeycombing, even if there is associated bronchiectasis (30). However, in patients with UIP, progression of ground-glass attenuation to honeycombing is common and indicates irreversible fibrosis (35).

Despite differences in distribution and CT pattern, the differential diagnosis between UIP and NSIP remains challenging, and surgical lung biopsy is required in all patients who do not present with the typical clinical and CT features of UIP.

## Cryptogenic Organizing Pneumonia

COP is an IIP with characteristic clinical and radiologic features. The histologic pattern of COP is organizing pneumonia, formerly referred to as bronchiolitis obliterans organizing pneumonia (BOOP). The term *BOOP* has been omitted to avoid confusion with airway diseases such as constrictive bronchiolitis (3).

### Clinical Features

The typical patient with COP has a mean age of 55 years. Women and men are equally affected and present with mild dyspnea, cough, and fever that have been developing over a few weeks (36).
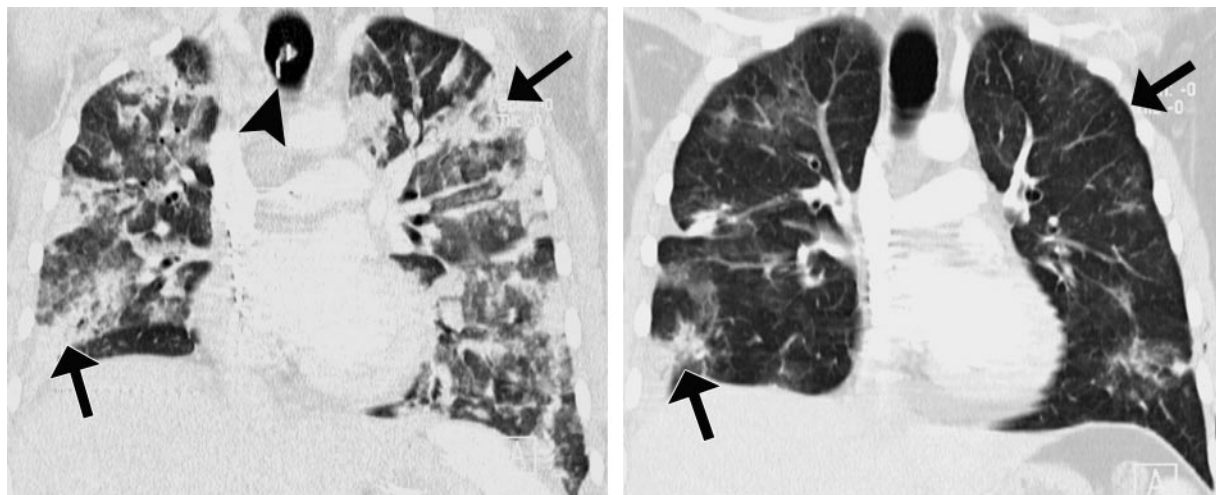
a.                                              b.

**Figure 14.**    COP in a 54-year-old woman. **(a)** Coronal CT image shows extensive bilateral peribronchial consolidation and ground-glass opacities (arrows). An endotracheal tube is present (arrowhead), indicating the need for mechanical ventilation. **(b)** CT image obtained after 3 weeks of corticosteroid and supportive treatment shows subtotal resolution of the lung abnormalities (arrows).
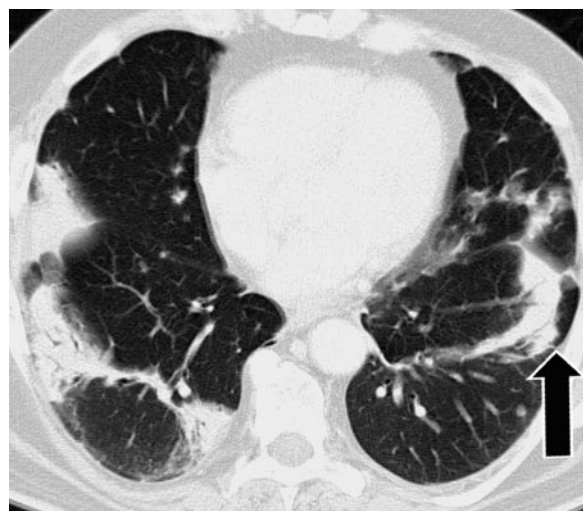


**Figure 15.**    COP in a 69-year-old man. High-resolution CT image shows peripherally located consolidation with air bronchograms and sparing of the subpleural space (arrow).

Patients typically report a respiratory tract infection preceding their symptoms, and antibiotics were commonly prescribed at a previous consultation (37). There is no association with cigarette smoking; in fact, most patients are nonsmokers or ex-smokers (3). The majority of patients recover completely after administration of corticosteroids, but relapses occur frequently within 3 months after corticosteroid therapy is reduced or stopped (38). As with the other interstitial pneumonias, the pattern of organizing pneumonia may occur in a wide variety of entities, notably in collagen vascular diseases and in infectious and drug-induced lung diseases (26,27). Therefore, the final

diagnosis of COP should be rendered only after exclusion of any other possible cause of organizing pneumonia.

### Histologic Features
The histologic hallmark of organizing pneumonia is the presence of granulation tissue polyps in the alveolar ducts and alveoli (Fig 12) (39). These fibroblast proliferations result from organization of inflammatory intraalveolar exudates (36). Typically, there is patchy lung involvement with preservation of lung architecture. The granulation tissue is all the same age and contains few inflammatory cells.

### Imaging Features
The chest radiograph in patients with COP usually shows unilateral or bilateral patchy consolidations that resemble pneumonic infiltrates (40). However, the consolidations in COP do not represent an active pneumonia but result from intraalveolar fibroblast proliferations, which may be associated with prior respiratory infection. Some patients present with nodular opacities on the chest radiograph. Lung volumes are preserved in most patients.

Frequently, the CT findings are far more extensive than expected from a review of the plain chest radiograph. The lung abnormalities show a characteristic peripheral or peribronchial distribution, and the lower lung lobes are more frequently involved (Figs 13, 14) (41). In some cases, the outermost subpleural area is spared (Fig 15) (42).
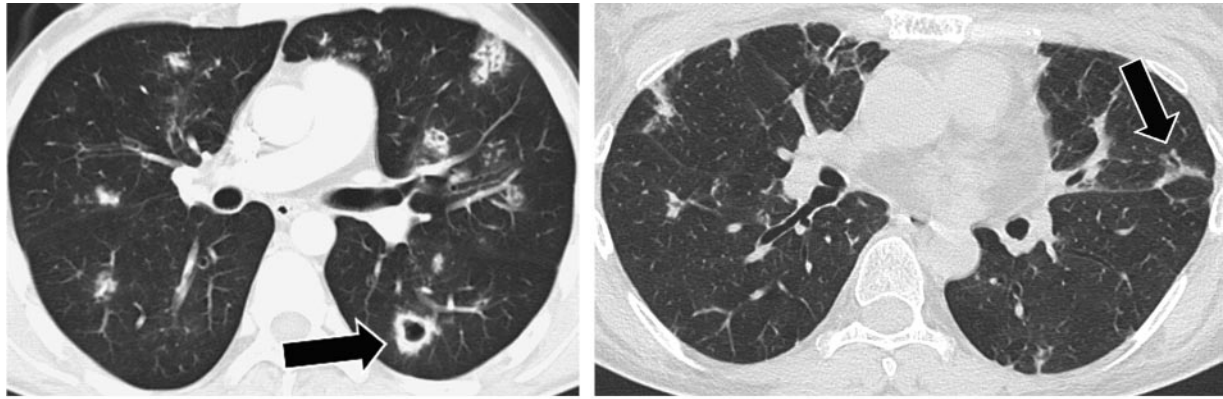
**Figure 16.** Atypical appearances of COP. **(a)** CT image shows bizarrely shaped nodules, some of which are cavitating (arrow). **(b)** CT image shows perilobular opacities that resemble thickened interlobular septa (arrow).

Typically, the appearance of the lung opacities varies from ground glass to consolidation; in the latter, air bronchograms and mild cylindrical bronchial dilatation are a common finding (41). These opacities have a tendency to migrate, changing location and size, even without treatment (42). They are of variable size, ranging from a few centimeters to an entire lobe.

In the appropriate clinical context, that is, consolidation that increases over several weeks despite antibiotics, the CT features of COP are often suggestive. However, apart from the typical imaging pattern of COP, other less specific imaging patterns can be encountered. These atypical imaging findings include irregular linear opacities, solitary focal lesions that resemble lung cancer, or multiple nodules that may cavitate (Fig 16) (43–45). In either case, the diagnosis should be confirmed with surgical lung biopsy. The role of transbronchial lung biopsy for diagnosis of COP is currently under evaluation (3).

## Respiratory Bronchiolitis–associated Interstitial Lung Disease

RB-ILD is a smoking-related interstitial lung disease and is thought to represent an exaggerated and symptomatic form of the histologically common and incidental finding of respiratory bronchiolitis. Because of the significant overlap in clinical, imaging, and histologic features between RB-ILD and DIP, these entities are considered a pathomorphologic continuum, representing different degrees of severity of the same disease process (46,47).
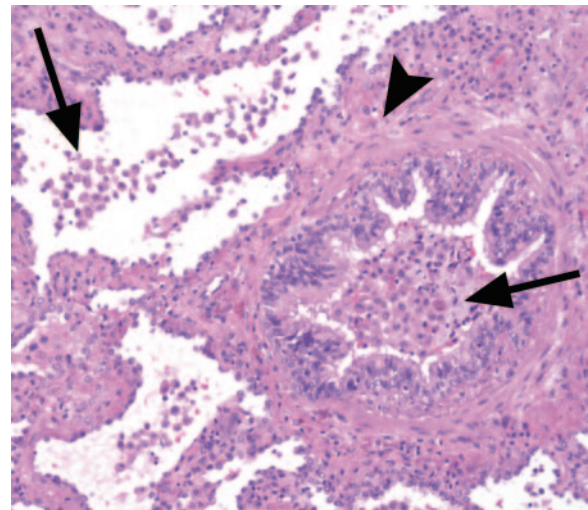


**Figure 17.** Histologic features of RB-ILD. Photomicrograph (original magnification, ×100; hematoxylin-eosin stain) shows pigmented alveolar macrophages in a terminal bronchiole and the adjacent alveoli (arrows). Moderate peribronchiolar inflammation and fibrosis are present (arrowhead).

### Clinical Features

Patients with RB-ILD are usually 30–40 years old and have an average smoking history of 30 pack-years (47). Men are affected nearly twice as often as women and present with mild dyspnea and cough. Smoking cessation is the most important component in the therapeutic management of RB-ILD. However, the majority of patients also receive corticosteroid therapy (48).

### Histologic Features

The histopathologic hallmark of RB-ILD is the intraluminal accumulation of pigmented macrophages centered around the respiratory bronchioles (Fig 17) (49). Mild peribronchiolar inflammation and fibrosis are usually present.
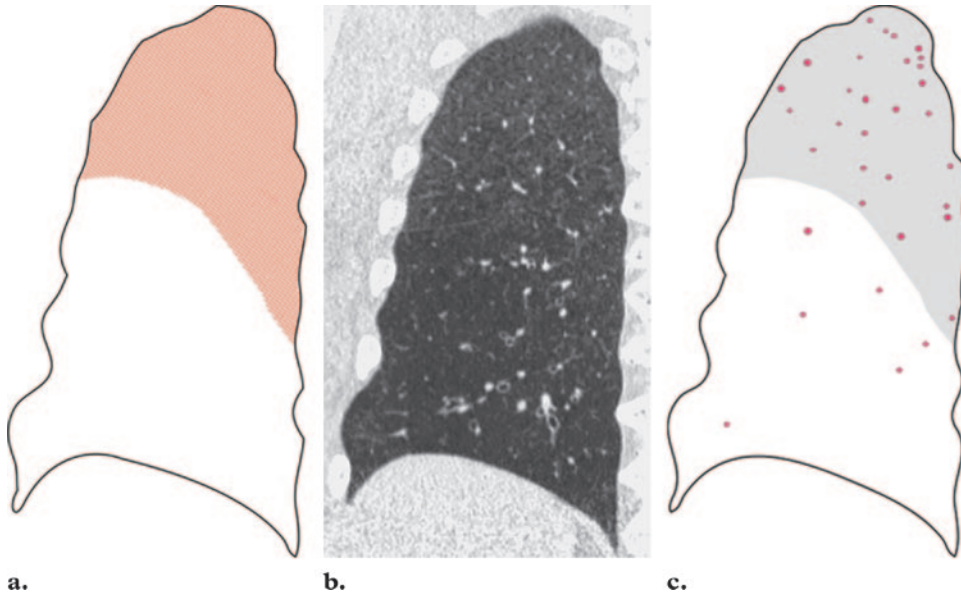
**a.**            **b.**            **c.**

**Figure 18.** Distribution **(a)**, CT image **(b)**, and CT pattern **(c)** of RB-ILD. RB-ILD has an upper lung predominance (red area in **a**). CT shows ground-glass opacity (gray area in **c**) and centrilobular nodules (red areas in **c**).



**Figure 19.** RB-ILD in a 44-year-old woman with a 20 pack-year smoking history. High-resolution CT image of the upper lung lobes shows centrilobular nodules (white arrows) and patchy ground-glass opacities (black arrow). Mild coexisting centrilobular emphysema is seen (arrowhead).

Findings in patients with RB-ILD cannot be differentiated histologically from those seen in asymptomatic patients with respiratory bronchiolitis.

### Imaging Features

The chest radiograph is insensitive for detection of RB-ILD and is often normal. Sometimes, bronchial wall thickening or reticular opacities can be seen (3,50).

The distribution at high-resolution CT is mostly diffuse (Fig 18) (46). The key high-resolution CT features of RB-ILD are centrilobular nodules in combination with ground-glass opacities and bronchial wall thickening (Fig 19) (47).

The ground-glass opacities have been shown to correlate with macrophage accumulation in alveolar ducts and alveolar spaces (51). The centrilobular nodules are presumably caused by the peribronchial distribution of the intraluminal infiltrates (52). Coexisting moderate centrilobular emphysema is common, given that most patients have a smoking history.

## Desquamative Interstitial Pneumonia

DIP is strongly associated with cigarette smoking and is considered to represent the end of a spectrum of RB-ILD. However, DIP also occurs in nonsmokers and has been related to a variety of conditions, including lung infections and exposure to organic dust (53,54).

### Clinical Features

For the majority of patients with DIP, the onset of symptoms is between 30 and 40 years of age. Men are affected about twice as often as women, and most patients are current or past smokers (average smoking history of 18 pack-years) (47).

With smoking cessation and corticosteroid therapy, the prognosis is good. Nevertheless, progressive disease with eventual death can occur, notably in patients with continued cigarette smoking (48).

### Histologic Features

The major histopathologic feature of DIP is the accumulation of pigmented macrophages and a few desquamated alveolar epithelial cells in the

**Figure 20.** Histologic features of DIP. Photomicrograph (original magnification, ×200; hematoxylin-eosin stain) shows diffuse filling of the alveolar spaces with alveolar macrophages and a few desquamated alveolar epithelial cells (arrow) (inset). Mild interstitial fibrosis is present (arrowhead).
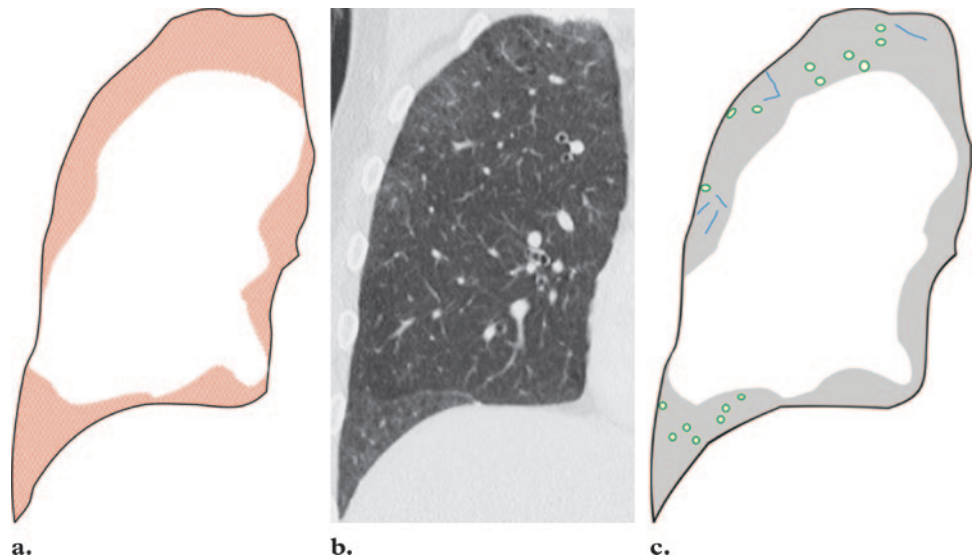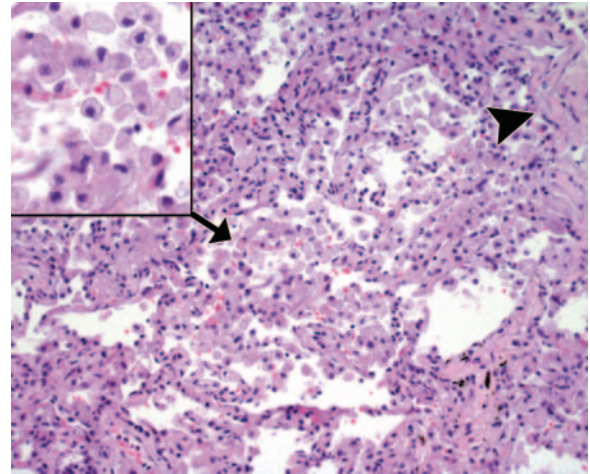


a.    b.    c.

**Figure 21.** Distribution **(a)**, CT image **(b)**, and CT pattern **(c)** of DIP. DIP has a peripheral predominance (red areas in **a**). CT shows ground-glass opacity (gray area in **c**), irregular linear opacities (blue areas in **c**), and cysts (green areas in **c**).

alveoli (Fig 20). As opposed to the bronchiolocentric distribution in RB-ILD, lung involvement in DIP is more diffuse and uniform (55). Usually, there is mild fibrosis in the interstitium. The more common DIP-like lung alterations seen in patients secondary to exposure to organic dust or in association with other IIPs, such as UIP, cannot be differentiated histologically from idiopathic DIP (56).

### Imaging Features
Chest radiographs of DIP are nonspecific and may reveal hazy opacities (57).

At high-resolution CT, DIP is characterized by diffuse ground-glass opacities, which correlate histologically with the spatially homogeneous intraalveolar accumulation of macrophages and thickening of alveolar septa (Fig 21) (58). Usually, there is a peripheral and lower lung lobe predominance (Fig 22) (59). Other frequent CT findings include spatially limited irregular linear opacities and small cystic spaces, which are indicative of fibrotic changes (Fig 23) (3).

Despite differences in the CT appearance of RB-ILD and DIP, imaging findings may overlap and may be indistinguishable from each other. To improve diagnostic accuracy, lung biopsy is required in all cases of suspected RB-ILD or DIP (3).

## Lymphoid Interstitial Pneumonia
As an idiopathic disease, LIP is exceedingly rare. It is far more common as a secondary disease in association with systemic disorders, most notably
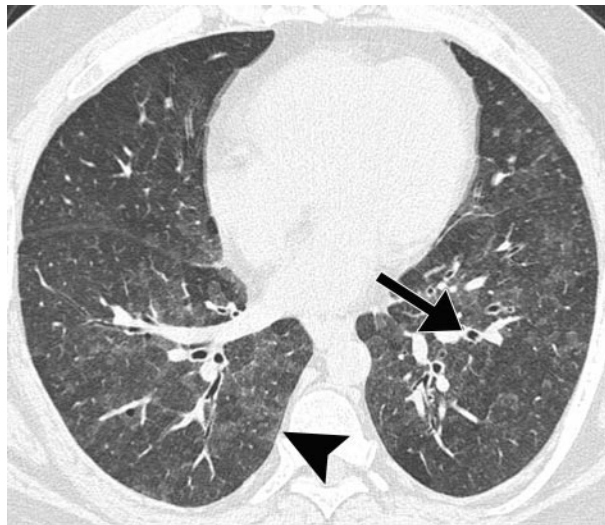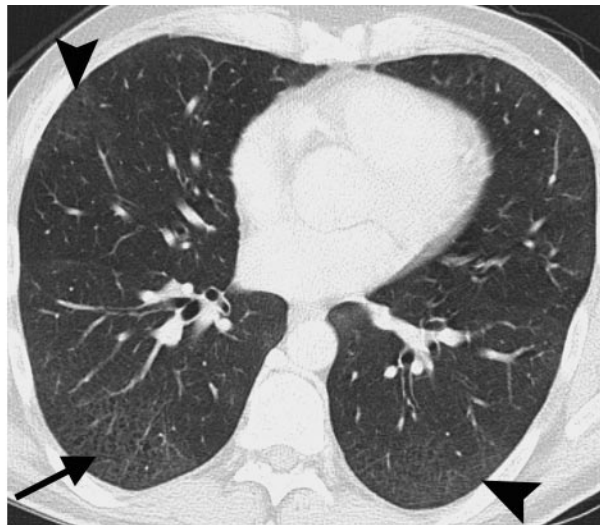
**Figures 22, 23.** **(22)** DIP in a 55-year-old man. High-resolution CT image of the lower lung lobes shows extensive bilateral ground-glass opacities (arrowhead). Coexisting moderate bronchial wall thickening is present (arrow). **(23)** DIP in a 43-year-old man with a history of smoking. High-resolution CT image of the lower lung zones shows patchy ground-glass opacities in both lungs, predominantly in the subpleural region (arrowheads). Small cystic spaces are present in these areas (arrow).
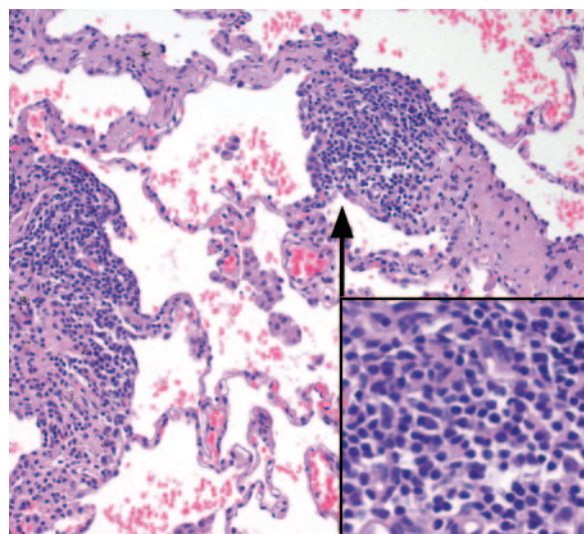


**Figure 24.** Histologic features of LIP. Photomicrograph (original magnification, ×200; hematoxylin-eosin stain) shows widening of alveolar septa by lymphoid infiltrates (arrow) (inset), which consist of mature lymphocytes, plasma cells, and histiocytes.

Sjögren syndrome, human immunodeficiency virus infection, and variable immunodeficiency syndromes (60).

## Clinical Features
LIP is more common in women than in men, and patients are usually in their fifth decade of life at presentation. They present with slowly progressive dyspnea and cough over a period of 3 or more years (3). Occasionally, patients report systemic symptoms, such as fever, night sweats, and weight loss. In the past, LIP was considered a pulmonary lymphoproliferative disorder, with subsequent progression to malignant lymphoma (61). However, many of these cases were reclassified as lymphoma from the outset, and only a small number of definite LIP cases seem to actually undergo malignant transformation (62). Corticosteroids are used in the therapy of LIP, but response is unpredictable and no controlled randomized treatment trials have been reported to date (60).

## Histologic Features
The LIP pattern is characterized by diffuse infiltration of the interstitium by lymphocytes, plasma cells, and histiocytes (Fig 24) (3). Reactive lymphoid follicles are often present and distributed along the peribronchiolar regions, which are highly inflamed. Although the predominant changes are interstitial, the airspaces display secondary changes, which range from compression by the interstitial infiltrates to proteinaceous fluid and macrophage collections (60).

## Imaging Features
The chest radiograph in patients with LIP reveals nonspecific findings, such as bilateral reticular, reticulonodular, or alveolar opacities.

High-resolution CT is the radiologic procedure of choice and shows bilateral abnormalities that are diffuse or have a lower lung predominance. The dominant high-resolution CT feature
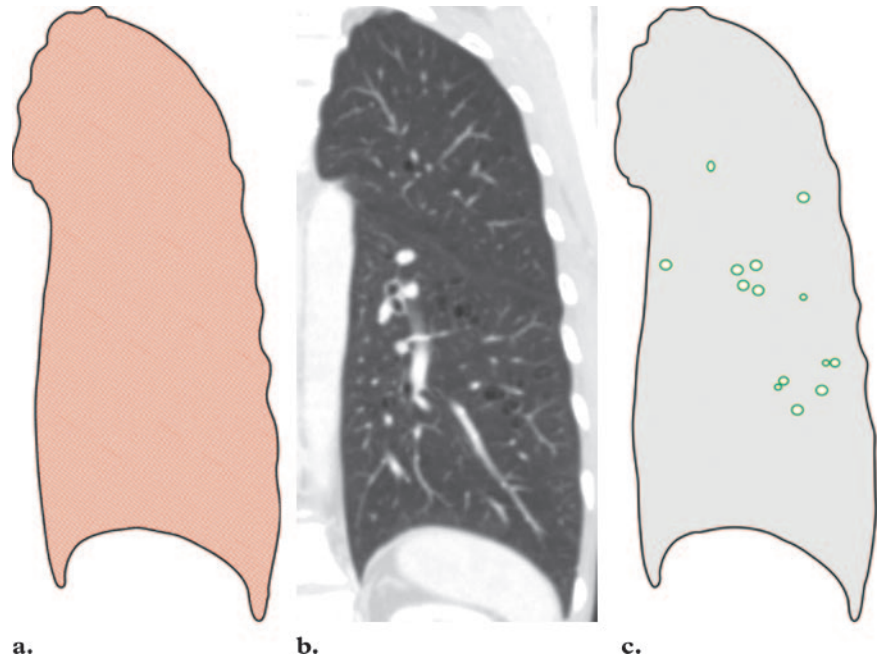
**Figure 25.** Distribution **(a)**, CT image **(b)**, and CT pattern **(c)** of LIP. The distribution is diffuse (red area in **a**). CT shows ground-glass opacity (gray area in **c**) and perivascular cysts (green areas in **c**).

a.                                    b.                                    c.



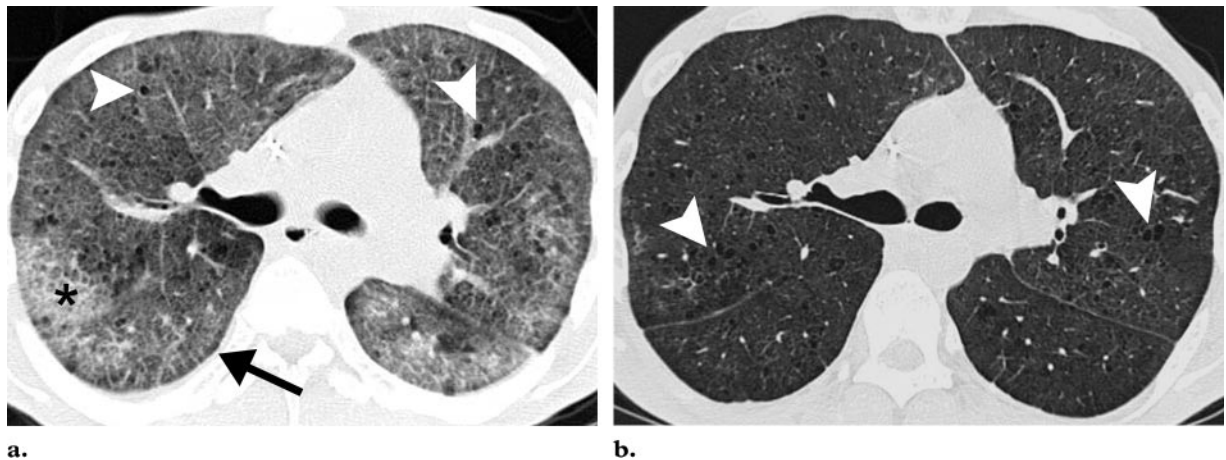a.                                                    b.

**Figure 26.** LIP in a 47-year-old woman. **(a)** High-resolution CT image shows diffuse ground-glass opacity (arrow) with multiple perivascular cysts (arrowheads) and reticular abnormalities (∗). **(b)** CT image obtained after corticosteroid therapy shows improvement, with partial resolution of the ground-glass and reticular opacities and better demarcation of the perivascular cysts (arrowheads).

in patients with LIP is ground-glass attenuation, which is related to the histologic evidence of diffuse interstitial inflammation (Fig 25) (63). Another frequent finding is thin-walled perivascular cysts (Fig 26) (64). In contrast to the subpleural, lower lung cystic changes in UIP, the cysts of LIP are usually within the lung parenchyma throughout the mid lung zones and presumably result from air trapping due to peribronchiolar cellular infiltration (64). In combination with ground-glass opacities, these cysts are highly suggestive of LIP. Occasionally, centrilobular nodules and septal thickening are seen (63).

## Acute Interstitial Pneumonia

AIP is the only entity among the IIPs with acute onset of symptoms. In most cases of AIP, the clinical and imaging criteria for acute respiratory distress syndrome are fulfilled.

### Clinical Features

Patients who present with AIP have a mean age of 50 years (3). Most patients develop severe dyspnea with a need for mechanical ventilation within less than 3 weeks (3). Typically, a history of viral-like illness exists. Men and women are equally affected, and cigarette smoking does not seem to increase the risk for development of AIP. Treatment is largely supportive and consists of
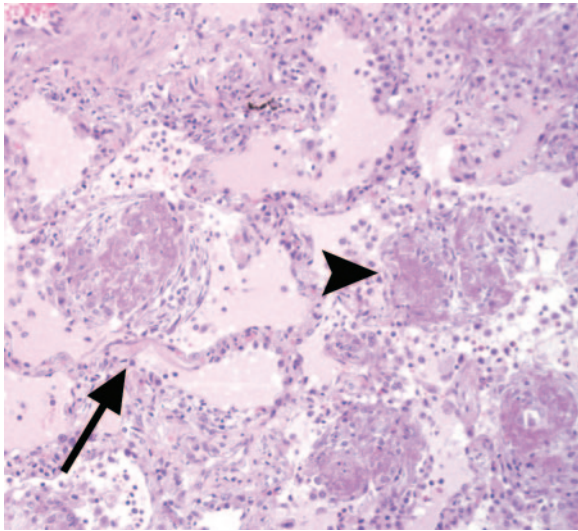
**Figure 27.** Histologic features of the exudative phase of AIP. The alveolar septa are diffusely thickened by hyaline membranes (arrow). Fibrin deposition and inflammatory cells are present in the alveoli (arrowhead).
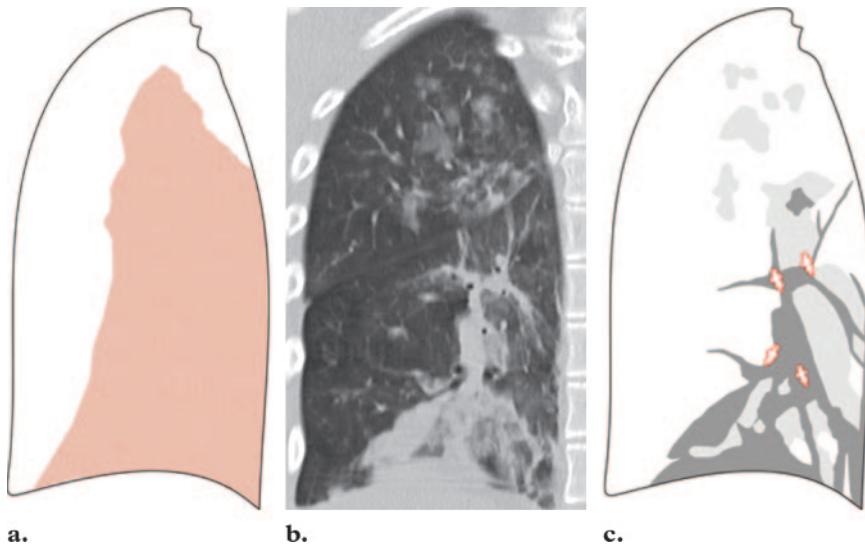


a.          b.          c.

**Figure 28.** Distribution **(a)**, CT image **(b)**, and CT pattern **(c)** of AIP. AIP has a basal predominance (red area in **a**). CT shows airspace consolidation (dark gray areas in **c**), ground-glass opacities (light gray areas in **c**), and bronchial dilatation (red areas in **c**).

oxygen supplementation. Corticosteroids seem to be effective in the early phase of disease (65). Nevertheless, the prognosis remains poor, with a mortality rate of 50% or more (3). Although recurrences of AIP have been described, most patients who survive the acute phase of the disease later progress to lung fibrosis (66,67).

### Histologic Features
The histologic pattern of AIP includes diffuse alveolar damage, which can be categorized into an early exudative phase and a chronic organizing phase, depending on the timing of the biopsy in relation to the lung insult (68). The exudative phase is characterized by interstitial and intraalveolar edema, formation of hyaline membranes, and diffuse alveolar infiltration by inflammatory cells (Fig 27). The organizing phase usually begins at the end of the first week after lung injury and is characterized by formation of granulation

tissue, which results in alveolar wall thickening. As opposed to the heterogeneous appearance of UIP, fibrotic changes in AIP are uniform and characterized by numerous fibroblasts but relatively little collagen deposition (69).

Histopathologic investigation is necessary for a definitive diagnosis of AIP. However, considering the fact that patients with AIP are often too ill to tolerate surgical lung biopsy, transbronchial biopsy seems to be sufficient (65).

### Imaging Features
The radiographic and high-resolution CT features of AIP are similar to those of acute respiratory distress syndrome; however, patients with AIP are more likely to have a symmetric, bilateral distribution with a lower lobe predominance (Fig 28) (70). The costophrenic angles are often
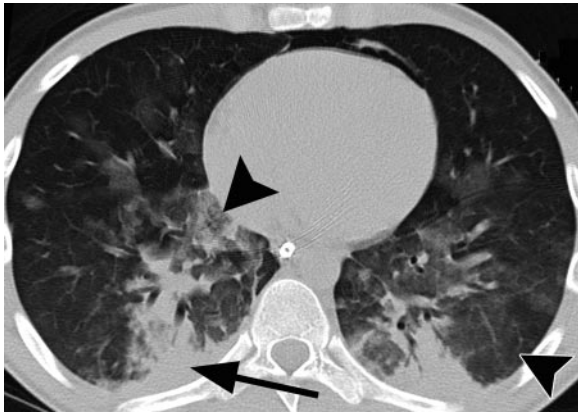
**Figure 29.**   Exudative phase of AIP in a 22-year-old man. High-resolution CT image shows bilateral ground-glass opacities (arrowheads) and consolidation (arrow) in the dependent areas of the lungs. The anterior zones of the lungs are relatively spared.
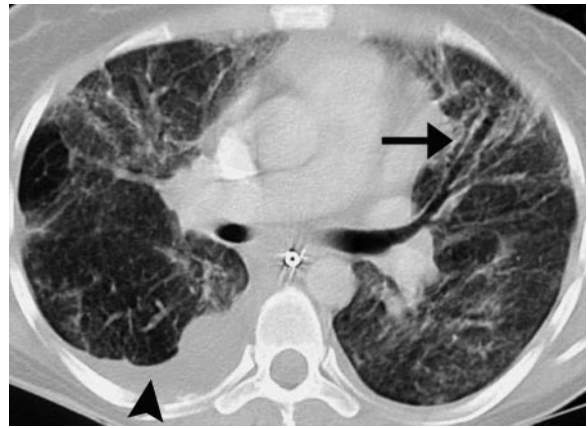


**Figure 30.**   Fibrotic phase of AIP in a 53-year-old woman who survived the acute phase of the disease. CT image shows fibrotic changes with traction bronchiectasis and architectural distortion predominantly in the nondependent areas of the lungs (arrow). A coexisting right pleural effusion is seen (arrowhead).

---

**Table 4**
**Ten Teaching Points for the Diagnostic Approach to IIPs**

IIPs are rare. Nevertheless, they are considered prototypes of the much more common secondary interstitial pneumonias that can be encountered in frequent disorders (eg, sarcoidosis, vasculitis, and connective tissue diseases). Therefore, radiologists should be familiar with their clinical and morphologic manifestations.

The classification of IIPs is based on histologic criteria, but those histologic patterns are closely associated with imaging patterns that correlate well with histologic findings.

Establishing the final diagnosis of IIPs requires close communication and interaction between clinicians, radiologists, and pathologists.

Diagnosis of IIPs is a dynamic process, and preliminary diagnostic assumptions may need to be revised during the diagnostic work-up.

High-resolution CT is indicated in virtually all patients suspected to have IIPs.

To ensure diagnostic accuracy, careful attention must be paid to use of an adequate high-resolution CT technique.

The key role of the radiologist is to identify patients with UIP and differentiate them from patients with other IIPs, because UIP has a substantially poorer prognosis than other IIPs.

In all patients suspected to have IIPs who do not show the typical clinical and radiologic features of UIP, surgical lung biopsy should be performed.

Biopsy specimens should always be obtained from more than one lobe, and high-resolution CT should serve as a guiding tool for determining the appropriate anatomic location of the biopsy site.

NSIP is an area of diagnostic uncertainty, and the term *NSIP* should be considered a provisional diagnosis until further characterization of this entity is achieved.

---

spared. In the early phase of AIP, ground-glass opacities are the dominant CT pattern and reflect the presence of alveolar septal edema and hyaline membranes (Fig 29) (69). Areas of consolidation are also present but are usually less extensive and limited to the dependent area of the lung (71). In the early phase, airspace consolidation results from intraalveolar edema and hemorrhage.

However, consolidations are also present in the fibrotic phase and then result from intraalveolar fibrosis (72). In the late phase of AIP, architectural distortion, traction bronchiectasis, and hon-

eycombing are the most striking CT features and are more severe in the nondependent areas of the lung (Fig 30) (72,73). This can be explained by the "protective" effect of atelectasis and consolidation on the dependent areas of the lung during the acute phase of disease, which attenuate the potential damage associated with mechanical ventilation (73).

## Conclusions

The ATS-ERS consensus statement of 2002 details the diagnostic approach to the IIPs. Table 4 summarizes 10 teaching points from this consensus statement that radiologists should be aware of

Teaching Point

Teaching Point

when dealing with these conditions. IIPs are associated with typical morphologic patterns. The CT appearances of UIP and COP may be diagnostic in the appropriate clinical context. However, there is substantial overlap in the CT appearances of the other IIPs. Therefore, accurate diagnosis of these disorders requires a dynamic interdisciplinary approach that correlates clinical, radiologic, and pathologic features.

## References

1. Katzenstein AL, Myers JL. Idiopathic pulmonary fibrosis: clinical relevance of pathologic classification. Am J Respir Crit Care Med 1998;157:1301–1315.
2. Liebow A. New concepts and entities in pulmonary disease. Monogr Pathol 1968;8:322–365.
3. American Thoracic Society; European Respiratory Society. American Thoracic Society/European Respiratory Society International Multidisciplinary Consensus Classification of the Idiopathic Interstitial Pneumonias. This joint statement of the American Thoracic Society (ATS), and the European Respiratory Society (ERS) was adopted by the ATS board of directors, June 2001 and by the ERS Executive Committee, June 2001. Am J Respir Crit Care Med 2002;165:277–304. [Published correction appears in Am J Respir Crit Care Med 2002;166:426.]
4. King TE Jr, Schwarz MI, Brown K, et al. Idiopathic pulmonary fibrosis: relationship between histopathologic features and mortality. Am J Respir Crit Care Med 2001;164:1025–1032.
5. du Bois RM, Wells AU. Cryptogenic fibrosing alveolitis/idiopathic pulmonary fibrosis. Eur Respir J Suppl 2001;32:43s–55s.
6. Hidalgo A, Franquet T, Gimenez A, Bordes R, Pineda R, Madrid M. Smoking-related interstitial lung diseases: radiologic-pathologic correlation. Eur Radiol 2006;16:2463–2470.
7. Taskar VS, Coultas DB. Is idiopathic pulmonary fibrosis an environmental disease? Proc Am Thorac Soc 2006;3:293–298.
8. Michaelson JE, Aguayo SM, Roman J. Idiopathic pulmonary fibrosis: a practical approach for diagnosis and management. Chest 2000;118:788–794.
9. Homma S, Sakamoto S, Kawabata M, et al. Cyclosporin treatment in steroid-resistant and acutely exacerbated interstitial pneumonia. Intern Med 2005;44:1144–1150.
10. Thabut G, Mal H, Castier Y, et al. Survival benefit of lung transplantation for patients with idiopathic pulmonary fibrosis. J Thorac Cardiovasc Surg 2003;126:469–475.
11. Monaghan H, Wells AU, Colby TV, du Bois RM, Hansell DM, Nicholson AG. Prognostic implications of histologic patterns in multiple surgical lung biopsies from patients with idiopathic interstitial pneumonias. Chest 2004;125:522–526.
12. Flaherty KR, Travis WD, Colby TV, et al. Histopathologic variability in usual and nonspecific interstitial pneumonias. Am J Respir Crit Care Med 2001;164:1722–1727.
13. Muller NL, Miller RR, Webb WR, Evans KG, Ostrow DN. Fibrosing alveolitis: CT-pathologic correlation. Radiology 1986;160:585–588.
14. Chandler PW, Shin MS, Friedman SE, Myers JL, Katzenstein AL. Radiographic manifestations of bronchiolitis obliterans with organizing pneumonia vs usual interstitial pneumonia. AJR Am J Roentgenol 1986;147:899–906.
15. Hunninghake GW, Lynch DA, Galvin JR, et al. Radiologic findings are strongly associated with a pathologic diagnosis of usual interstitial pneumonia. Chest 2003;124:1215–1223.
16. Johkoh T, Muller NL, Cartier Y, et al. Idiopathic interstitial pneumonias: diagnostic accuracy of thin-section CT in 129 patients. Radiology 1999; 211:555–560.
17. MacDonald SL, Rubens MB, Hansell DM, et al. Nonspecific interstitial pneumonia and usual interstitial pneumonia: comparative appearances at and diagnostic accuracy of thin-section CT. Radiology 2001;221:600–605.
18. Raghu G, Mageto YN, Lockhart D, Schmidt RA, Wood DE, Godwin JD. The accuracy of the clinical diagnosis of new-onset idiopathic pulmonary fibrosis and other interstitial lung disease: a prospective study. Chest 1999;116:1168–1174.
19. Hunninghake GW, Zimmerman MB, Schwartz DA, et al. Utility of a lung biopsy for the diagnosis of idiopathic pulmonary fibrosis. Am J Respir Crit Care Med 2001;164:193–196.
20. Flaherty KR, Thwaite EL, Kazerooni EA, et al. Radiological versus histological diagnosis in UIP and NSIP: survival implications. Thorax 2003;58: 143–148.
21. Travis WD, Matsui K, Moss J, Ferrans VJ. Idiopathic nonspecific interstitial pneumonia: prognostic significance of cellular and fibrosing patterns—survival comparison with usual interstitial pneumonia and desquamative interstitial pneumonia. Am J Surg Pathol 2000;24:19–33.
22. Riha RL, Duhig EE, Clarke BE, Steele RH, Slaughter RE, Zimmerman PV. Survival of patients with biopsy-proven usual interstitial pneumonia and nonspecific interstitial pneumonia. Eur Respir J 2002;19:1114–1118.
23. Latsi PI, du Bois RM, Nicholson AG, et al. Fibrotic idiopathic interstitial pneumonia: the prognostic value of longitudinal functional trends. Am J Respir Crit Care Med 2003;168: 531–537.
24. Martinez FJ. Idiopathic interstitial pneumonias: usual interstitial pneumonia versus nonspecific interstitial pneumonia. Proc Am Thorac Soc 2006;3:81–95.
25. Daniil ZD, Gilchrist FC, Nicholson AG, et al. A histologic pattern of nonspecific interstitial pneumonia is associated with a better prognosis than usual interstitial pneumonia in patients with cryptogenic fibrosing alveolitis. Am J Respir Crit Care Med 1999;160:899–905.
26. Kim EA, Lee KS, Johkoh T, et al. Interstitial lung diseases associated with collagen vascular diseases: radiologic and histopathologic findings. RadioGraphics 2002;22(spec no):S151–S165.

RadioGraphics

27. Rossi SE, Erasmus JJ, McAdams HP, Sporn TA, Goodman PC. Pulmonary drug toxicity: radiologic and pathologic manifestations. RadioGraphics 2000;20:1245–1259.

28. Katzenstein AL, Fiorelli RF. Nonspecific interstitial pneumonia/fibrosis: histologic features and clinical significance. Am J Surg Pathol 1994;18:136–147.

29. Johkoh T, Muller NL, Colby TV, et al. Nonspecific interstitial pneumonia: correlation between thin-section CT findings and pathologic subgroups in 55 patients. Radiology 2002;225:199–204.

30. Akira M, Inoue G, Yamamoto S, Sakatani M. Non-specific interstitial pneumonia: findings on sequential CT scans of nine patients. Thorax 2000;55:854–859.

31. Kim EY, Lee KS, Chung MP, Kwon OJ, Kim TS, Hwang JH. Nonspecific interstitial pneumonia with fibrosis: serial high-resolution CT findings with functional correlation. AJR Am J Roentgenol 1999;173:949–953.

32. Wells AU, Desai SR, Rubens MB, et al. Idiopathic pulmonary fibrosis: a composite physiologic index derived from disease extent observed by computed tomography. Am J Respir Crit Care Med 2003;167:962–969.

33. Desai SR, Veeraraghavan S, Hansell DM, et al. CT features of lung disease in patients with systemic sclerosis: comparison with idiopathic pulmonary fibrosis and nonspecific interstitial pneumonia. Radiology 2004;232:560–567.

34. Do KH, Lee JS, Colby TV, Kitaichi M, Kim DS. Nonspecific interstitial pneumonia versus usual interstitial pneumonia: differences in the density histogram of high-resolution CT. J Comput Assist Tomogr 2005;29:544–548.

35. Remy-Jardin M, Giraud F, Remy J, Copin MC, Gosselin B, Duhamel A. Importance of ground-glass attenuation in chronic diffuse infiltrative lung disease: pathologic-CT correlation. Radiology 1993;189:693–698.

36. Cordier JF. Organising pneumonia. Thorax 2000;55:318–328.

37. Cordier JF, Loire R, Brune J. Idiopathic bronchiolitis obliterans organizing pneumonia: definition of characteristic clinical profiles in a series of 16 patients. Chest 1989;96:999–1004.

38. Lazor R, Vandevenne A, Pelletier A, Leclerc P, Court-Fortune I, Cordier JF. Cryptogenic organizing pneumonia: characteristics of relapses in a series of 48 patients. The Groupe d'Etudes et de Recherche sur les Maladies "Orphelines" Pulmonaires (GERM"O"P). Am J Respir Crit Care Med 2000;162:571–577.

39. Myers JL, Colby TV. Pathologic manifestations of bronchiolitis, constrictive bronchiolitis, cryptogenic organizing pneumonia, and diffuse panbronchiolitis. Clin Chest Med 1993;14:611–622.

40. Muller NL, Guerry-Force ML, Staples CA, et al. Differential diagnosis of bronchiolitis obliterans with organizing pneumonia and usual interstitial pneumonia: clinical, functional, and radiologic findings. Radiology 1987;162:151–156.

41. Lee KS, Kullnig P, Hartman TE, Muller NL. Cryptogenic organizing pneumonia: CT findings in 43 patients. AJR Am J Roentgenol 1994;162:543–546.

42. Izumi T, Kitaichi M, Nishimura K, Nagai S. Bronchiolitis obliterans organizing pneumonia: clinical features and differential diagnosis. Chest 1992;102:715–719.

43. Akira M, Yamamoto S, Sakatani M. Bronchiolitis obliterans organizing pneumonia manifesting as multiple large nodules or masses. AJR Am J Roentgenol 1998;170:291–295.

44. Bouchardy LM, Kuhlman JE, Ball WC Jr, Hruban RH, Askin FB, Siegelman SS. CT findings in bronchiolitis obliterans organizing pneumonia (BOOP) with radiographic, clinical, and histologic correlation. J Comput Assist Tomogr 1993;17:352–357.

45. Haro M, Vizcaya M, Texido A, Aguilar X, Arevalo M. Idiopathic bronchiolitis obliterans organizing pneumonia with multiple cavitary lung nodules. Eur Respir J 1995;8:1975–1977.

46. Moon J, du Bois RM, Colby TV, Hansell DM, Nicholson AG. Clinical significance of respiratory bronchiolitis on open lung biopsy and its relationship to smoking related interstitial lung disease. Thorax 1999;54:1009–1014.

47. Heyneman LE, Ward S, Lynch DA, Remy-Jardin M, Johkoh T, Muller NL. Respiratory bronchiolitis, respiratory bronchiolitis-associated interstitial lung disease, and desquamative interstitial pneumonia: different entities or part of the spectrum of the same disease process? AJR Am J Roentgenol 1999;173:1617–1622.

48. Ryu JH, Myers JL, Capizzi SA, Douglas WW, Vassallo R, Decker PA. Desquamative interstitial pneumonia and respiratory bronchiolitis-associated interstitial lung disease. Chest 2005;127: 178–184.

49. Myers JL, Veal CF Jr, Shin MS, Katzenstein AL. Respiratory bronchiolitis causing interstitial lung disease: a clinicopathologic study of six cases. Am Rev Respir Dis 1987;135:880–884.

50. Ryu JH, Colby TV, Hartman TE, Vassallo R. Smoking-related interstitial lung diseases: a concise review. Eur Respir J 2001;17:122–132.

51. Remy-Jardin M, Remy J, Boulenguez C, Sobaszek A, Edme JL, Furon D. Morphologic effects of cigarette smoking on airways and pulmonary parenchyma in healthy adult volunteers: CT evaluation and correlation with pulmonary function tests. Radiology 1993;186:107–115.

52. Howling SJ, Hansell DM, Wells AU, Nicholson AG, Flint JD, Muller NL. Follicular bronchiolitis: thin-section CT and histologic findings. Radiology 1999;212:637–642.

53. Sung SA, Ko GJ, Kim JY, et al. Desquamative interstitial pneumonia associated with concurrent cytomegalovirus and Aspergillus pneumonia in a renal transplant recipient. Nephrol Dial Transplant 2005;20:635–638.

54. Kern DG, Kuhn C 3rd, Ely EW, et al. Flock worker's lung: broadening the spectrum of clinicopathology, narrowing the spectrum of suspected etiologies. Chest 2000;117:251–259.

55. Yousem SA, Colby TV, Gaensler EA. Respiratory bronchiolitis-associated interstitial lung disease and its relationship to desquamative interstitial pneumonia. Mayo Clin Proc 1989;64:1373–1380.

56. Fraig M, Shreesha U, Savici D, Katzenstein AL. Respiratory bronchiolitis: a clinicopathologic study in current smokers, ex-smokers, and never-smokers. Am J Surg Pathol 2002;26:647–653.

57. Feigin DS, Friedman PJ. Chest radiography in desquamative interstitial pneumonitis: a review of 37 patients. AJR Am J Roentgenol 1980;134:91–99.

58. Lynch DA, Travis WD, Muller NL, et al. Idiopathic interstitial pneumonias: CT features. Radiology 2005;236:10–21.

59. Akira M, Yamamoto S, Hara H, Sakatani M, Ueda E. Serial computed tomographic evaluation in desquamative interstitial pneumonia. Thorax 1997;52:333–337.

60. Swigris JJ, Berry GJ, Raffin TA, Kuschner WG. Lymphoid interstitial pneumonia: a narrative review. Chest 2002;122:2150–2164.

61. Banerjee D, Ahmad D. Malignant lymphoma complicating lymphocytic interstitial pneumonia: a monoclonal B-cell neoplasm arising in a polyclonal lymphoproliferative disorder. Hum Pathol 1982;13:780–782.

62. Addis BJ, Hyjek E, Isaacson PG. Primary pulmonary lymphoma: a re-appraisal of its histogenesis and its relationship to pseudolymphoma and lymphoid interstitial pneumonia. Histopathology 1988;13:1–17.

63. Johkoh T, Muller NL, Pickford HA, et al. Lymphocytic interstitial pneumonia: thin-section CT findings in 22 patients. Radiology 1999;212:567–572.

64. Ichikawa Y, Kinoshita M, Koga T, Oizumi K, Fujimoto K, Hayabuchi N. Lung cyst formation in lymphocytic interstitial pneumonia: CT features. J Comput Assist Tomogr 1994;18:745–748.

65. Akira M, Hamada H, Sakatani M, Kobayashi C, Nishioka M, Yamamoto S. CT findings during phase of accelerated deterioration in patients with idiopathic pulmonary fibrosis. AJR Am J Roentgenol 1997;168:79–83.

66. Vourlekis JS, Brown KK, Cool CD, et al. Acute interstitial pneumonitis: case series and review of the literature. Medicine (Baltimore) 2000;79:369–378.

67. Olson J, Colby TV, Elliott CG. Hamman-Rich syndrome revisited. Mayo Clin Proc 1990;65: 1538–1548.

68. Savici D, Katzenstein AL. Diffuse alveolar damage and recurrent respiratory failure: report of 6 cases. Hum Pathol 2001;32:1398–1402.

69. Johkoh T, Muller NL, Taniguchi H, et al. Acute interstitial pneumonia: thin-section CT findings in 36 patients. Radiology 1999;211:859–863.

70. Bonaccorsi A, Cancellieri A, Chilosi M, et al. Acute interstitial pneumonia: report of a series. Eur Respir J 2003;21:187–191.

71. Akira M. Computed tomography and pathologic findings in fulminant forms of idiopathic interstitial pneumonia. J Thorac Imaging 1999;14:76–84.

72. Ichikado K, Johkoh T, Ikezoe J, et al. Acute interstitial pneumonia: high-resolution CT findings correlated with pathology. AJR Am J Roentgenol 1997;168:333–338.

73. Desai SR, Wells AU, Rubens MB, Evans TW, Hansell DM. Acute respiratory distress syndrome: CT abnormalities at long-term follow-up. Radiology 1999;210:29–35.

# What Every Radiologist Should Know about Idiopathic Interstitial Pneumonias

*Christina Mueller-Mang, MD et al*

**Page 597**
The classification of IIPs is based on histologic criteria, but each histologic pattern is associated with a characteristic computed tomography (CT) pattern that, provided an adequate CT technique is used, correlates well with histologic findings (Table 2) (3).

**Page 599**
Therefore, UIP should be considered in patients who present with low lung volumes, subpleural reticular opacities, macrocystic honeycombing, and traction bronchiectasis, the extent of which increases from the apex to the bases of the lungs (Fig 4).

**Page 600**
NSIP is associated with a variety of imaging and histologic findings, and the diagnostic approach is highly challenging. However, the distinction of NSIP from UIP is more than academic, given the better response to corticosteroids seen in a subgroup of patients with NSIP (22,23).

**Page 613**
The CT appearances of UIP and COP may be diagnostic in the appropriate clinical context.

**Page 613**
Therefore, accurate diagnosis of these disorders requires a dynamic interdisciplinary approach that correlates clinical, radiologic, and pathologic features.